

The linear spin-up of a strongly stratified fluid of small Prandtl number

By ALFRED CLARK, JR

Department of Mechanical and Aerospace Sciences, University of
Rochester, New York

(Received 22 January 1973)

The spin-up of a thermally stratified Boussinesq fluid in a circular cylinder with insulated side walls is analysed under the conditions of strong stratification (Brunt–Väisälä frequency $N \gg$ rotation frequency Ω) and small Prandtl number. An earlier paper (Sakurai, Clark & Clark 1971) showed that complete spin-up is achieved in the Eddington–Sweet time. The present work considers in detail the spin-up transients corresponding to shorter time scales.

The analysis reveals a complicated system of merging and bifurcating horizontal layers in the interior flow. Following the spin-up of the cylindrical container, a rotational shear layer, of the kind discovered by Holton (1965), forms near each horizontal boundary. At the same time, a thermal boundary layer begins diffusing outward from each boundary. When the thermal layer reaches the shear layer, the two merge and form a higher order layer, which diffuses at a rate proportional to $t^{\frac{1}{2}}$. At a later time, the layer splits into a steady layer and another diffusing layer, this time following a $t^{\frac{3}{2}}$ law. One important conclusion from the analysis is that the lifetime of the rotational shear layer is not great: it is of order $(\Omega/N)^2 (R^2/\chi)$, where R is the radius of the cylinder and χ is the thermal diffusivity.

The problem of computing the angular velocity from the poorly converging series is dealt with in some detail, and graphs are given of representative values. The results show that, for spin-up, there are appreciable adverse gradients of angular momentum near the side wall, and thus there is some question about the stability of the spin-up configuration.

Finally, a discussion is given of continuous spin-up of the container and the results are applied qualitatively to the solar spin-down problem. The principal conclusion is that the Ekman time scale is unimportant in the solar case.

1. Introduction

A problem of continuing interest in the theory of rotating fluids is the spin-up problem, in which one analyses the response of an enclosed rotating fluid to an increase in the angular velocity of the container. A basic parameter in the process is the Ekman number $E = \nu/(L^2\Omega)$, where ν is the kinematic viscosity, Ω is the angular velocity and L is a characteristic container dimension. The fundamental analysis of Greenspan & Howard (1963) showed that, for small E , the primary

mechanism for spinning up the contained fluid is the transport of angular momentum by secondary circulations. The circulations are generated in Ekman boundary layers which form on the non-vertical portions of the container wall. For an unstratified fluid, the angular velocity remains uniform in space while evolving on the Ekman time scale

$$t_{EK} = \Omega^{-1}E^{-\frac{1}{2}}, \quad (1)$$

which is much shorter than the viscous diffusion time

$$t_V = L^2/\nu = \Omega^{-1}E^{-1}. \quad (2)$$

The situation for a stratified fluid is more complicated, sufficiently so to have caused a lively controversy for several years. The controversy has subsided, and the original picture emerging from Holton's (1965) work has been firmly established by the analyses of Walin (1969) and Sakurai (1969). According to their work, the secondary circulations still operate on a time scale comparable with t_{EK} , but in the case of strong stratification, they are confined to regions near the boundary. The thickness of these regions is of order

$$\delta_{RS} = L\Omega/N, \quad (3)$$

where N is the Brunt-Väisälä frequency. Thus $\delta_{RS} \ll L$ if $\Omega \ll N$, which we assume throughout this paper. The result of the circulations is a quasi-static, spatially non-uniform spin-up, confined to these layers. In what follows, we shall call these rotational shear layers *RS* layers for short. The slow transition from this state of non-uniform rotation to the final state of uniform rotation comes about only because of the direct action of dissipative effects in the interior. The effects are viscous diffusion, with a time scale $t_V = L^2/\nu$, and thermally driven circulations, acting on the Eddington-Sweet time scale

$$t_{ES} = (N/\Omega)^2(L^2/\chi), \quad (4)$$

where χ is the thermal diffusivity. The relative importance of these mechanisms depends on the ratio

$$t_{ES}/t_V = (N/\Omega)^2 \mathcal{P}, \quad \mathcal{P} = \nu/\chi. \quad (5)$$

If the Prandtl number \mathcal{P} is sufficiently small, the final approach to uniform rotation is determined by the thermally driven circulations, and that is the case considered here. We also assume that the Eddington-Sweet time is longer than the Ekman time. Thus the parameter restrictions are

$$t_{EK} \ll t_{ES} \ll t_V, \quad \text{or} \quad E^{\frac{1}{2}} \ll (N/\Omega)^2 \mathcal{P} \ll 1. \quad (6)$$

This parameter range is of particular interest in astrophysical problems, since (6) typically is satisfied in stellar interiors.

Small Prandtl number spin-up has been analysed by Sakurai *et al.* (1971, called I hereafter). Their calculations showed that complete spin-up occurs on the Eddington-Sweet scale t_{ES} . Paper I did not, however, consider in any detail the spin-up transients corresponding to shorter time scales. The object of this paper is to study the surprisingly rich transient structure of the spin-up

flow. What emerges from the analysis is a complicated set of coalescing and bifurcating layers. An understanding of these layers is important for several reasons. In the first place, they must be accounted for in numerical work of the kind necessary for nonlinear problems. In the second place, such layers are of importance in the question of stability in spin-up. In addition to studying the layer structure, the present paper clarifies the role of Ekman pumping in stratified spin-up. A specific conclusion of some interest is that the Ekman time scale is of no importance in the problem of solar rotation.

As in I, the calculations here are carried out for a cylindrical geometry, primarily because it is the least complicated geometry which is still interesting for stratified spin-up. (Parallel disks, although simpler, are completely atypical (Sakurai 1969).) Some confidence in the suggestion that the cylinder is typical may be gained by comparing the work of Walin (1969) and Sakurai (1969) (cylindrical geometry) with the work of Clark *et al.* (1971) (spherical geometry). The restriction to times shorter than t_{ES} allows a further simplification in the geometry, since, in that case, the region of significant flow does not extend to the centre of the cylinder. Thus the layer structures on each end of the cylinder do not overlap and we can study the simpler case of the structure at one end of a semi-infinite cylinder.

The problem is formulated in § 2 and then solved by means of a radial expansion in Bessel functions and a Laplace transform in time. Section 3 gives a detailed qualitative picture of the complicated transient layer structure and a discussion of the role of Ekman pumping. In § 4, numerical results are given for impulsive spin-up. At the expense of some redundancy, a summary of the many time scales is given in § 5. Section 6 contains a discussion of the solar spin-down problem in the light of the present work. Sections 5 and 6 are reasonably self-contained, so that the reader interested only in the conclusions can skip the analysis of §§ 2–4.

2. Basic equations

2.1. Formulation

We consider a semi-infinite circular cylinder of radius R . The interior ($0 < z < \infty$, $0 < r < R$) contains a stably stratified Boussinesq fluid. Initially, the fluid and cylinder are in uniform rotation with angular velocity Ω . Then the container angular velocity is suddenly increased to $(1 + \epsilon)\Omega$, where ϵ , the Rossby number, is small. The side wall ($r = R$) is insulated and the end plate ($z = 0$) is maintained at a fixed temperature. The problem is to compute the subsequent evolution of the fluid's angular velocity. It is worth noting that, qualitatively, the results are not sensitive to the thermal boundary condition on the side wall. This is shown clearly by the results in I, where both insulated and fixed-temperature side walls were analysed.

In the formulation of the problem, we shall omit the thermally driven circulations associated with the centrifugal force (Barcilon & Pedlosky 1967). Such circulations give rise to non-uniform steady states of rotation. It is not hard to show that, in a linear theory, the transients connecting two such equilibrium

states are governed by the equations used in this paper. Thus, for the sake of simplicity, we omit the centrifugal force terms.

The linearized equations in the Boussinesq approximation are the equation of motion

$$\partial \mathbf{U} / \partial t = -2\boldsymbol{\Omega} \times \mathbf{U} - \alpha T \mathbf{g} - \rho^{-1} \nabla P + \nu \nabla^2 \mathbf{U}, \quad (7)$$

the continuity equation

$$\nabla \cdot \mathbf{U} = 0 \quad (8)$$

and the thermal equation

$$\partial T / \partial t + \beta W = \chi \nabla^2 T. \quad (9)$$

Here \mathbf{U} is the velocity relative to the uniform rotation $\boldsymbol{\Omega}$ (in the positive z direction), α is the coefficient of thermal expansion, T is the perturbation temperature, \mathbf{g} is the acceleration due to gravity (in the negative z direction), ρ is the constant mean density, P is the perturbation pressure, ν is the kinematic viscosity, χ is the thermal diffusivity, β is the constant temperature gradient in the unperturbed fluid and W is the vertical component of \mathbf{U} . We can satisfy (8) and exploit the condition of axisymmetry by introducing a stream function ψ , defined so that

$$\mathbf{U} = -\nabla \times (\psi \mathbf{e}_\phi) + V \mathbf{e}_\phi, \quad (10)$$

where \mathbf{e}_ϕ is the azimuthal unit vector and V is the azimuthal velocity. Both ψ and V are functions of the radial co-ordinate r , the vertical co-ordinate z and the time t . From (7) we get the following equations for ψ and V :

$$\mathcal{L} \left(\frac{\partial \psi}{\partial t} - \nu \mathcal{L} \psi \right) = 2\Omega \frac{\partial V}{\partial z} - \alpha g \frac{\partial T}{\partial r} \quad (11)$$

and

$$\partial V / \partial t - \nu \mathcal{L} V = -2\Omega \partial \psi / \partial z, \quad (12)$$

where

$$\mathcal{L} = \nabla^2 - r^{-2}. \quad (13)$$

The thermal equation (9) becomes

$$\frac{\partial T}{\partial t} - \chi \nabla^2 T = \frac{\beta}{r} \frac{\partial}{\partial r} (r\psi). \quad (14)$$

The boundary and initial conditions are

$$\psi = \partial \psi / \partial z = T = V - \epsilon \Omega r = 0 \quad \text{at } z = 0, \quad (15)$$

$$\psi = \partial \psi / \partial r = \partial T / \partial r = V - \epsilon \Omega R = 0 \quad \text{at } r = R \quad (16)$$

and

$$\psi = V = T = 0 \quad \text{at } t = 0. \quad (17)$$

2.2. Interior equations

Significant simplifications may be introduced using boundary-layer theory. A systematic approach, involving expansions in powers of the Ekman number, is given in detail in I. Rather than repeat that lengthy analysis, we give a brief heuristic treatment here. The basic idea is that the viscous terms are important only in thin boundary layers. Thus they need be retained only in the boundary-

layer analysis (given in I) and not in the equations for the interior flow. The thermal diffusion term, however, ($\chi \nabla^2 T$ in (14)) must be retained in the interior equations in the case of small Prandtl number. We may simplify (11) since the circulations (characterized by ψ) are very slow and have negligible inertia. Thus the term $\mathcal{L}(\partial\psi/\partial t)$ may be dropped. The resulting interior equations are

$$2\Omega \partial V/\partial z = \alpha g \partial T/\partial r, \tag{18}$$

$$\partial V/\partial t = -2\Omega \partial\psi/\partial z \tag{19}$$

and the thermal equation, which still has the form (14).

We now put the equations in dimensionless form. It is convenient to introduce the Brunt-Väisälä frequency N and the stratification parameter S , defined by $N^2 = \alpha\beta g$ and $S = (N/\Omega)^2$. As was mentioned in §1, we take $S \gg 1$. The proper scaling for the equations is easily obtained from the results of I. For the length scale, we choose the radius R of the cylinder. For the time scale, we take the Eddington-Sweet time $t_{ES} = SR^2/\chi$. The azimuthal velocity is scaled by $\epsilon R\Omega$ and the stream function by $\epsilon\chi/S$. The temperature scale is $\epsilon R\Omega^2/\alpha g$. Then the interior equations (with the same notation for dimensionless quantities) are

$$2\partial V/\partial z = \partial T/\partial r, \tag{20}$$

$$\partial V/\partial t = -2\partial\psi/\partial z \tag{21}$$

and
$$\frac{1}{S} \frac{\partial T}{\partial t} - \nabla^2 T = \frac{1}{r} \frac{\partial}{\partial r} (r\psi). \tag{22}$$

The solutions of these equations must be supplemented by boundary-layer corrections in order to satisfy the boundary conditions (15) and (16). The result of such an analysis (see I) is, conveniently, a set of effective boundary conditions to be imposed directly on the interior flow:

$$2\lambda\psi + V = r, \quad T = 0 \quad \text{at} \quad z = 0, \tag{23}, (24)$$

and
$$\partial T/\partial r + \psi = 0 \quad \text{at} \quad r = 1. \tag{25}$$

The condition (23) comes from the Ekman-layer analysis, and

$$\lambda = (\chi/RS)(\nu\Omega)^{-\frac{1}{2}} = t_{EK}/t_{ES}, \tag{26}$$

where, by our earlier assumption (6), $\lambda \ll 1$. The condition (24) is simply the true thermal boundary condition imposed directly on the interior flow—to be expected, since the thermal diffusion term is present in the interior equations. The condition (25) is the statement that the radial component of the total heat flux (convective plus conductive) vanishes at the edge of the interior flow.

The formulation is completed by the initial conditions

$$T = V = 0 \quad \text{for} \quad t = 0. \tag{27}$$

The initial condition on ψ is dropped, consistent with the neglect of the inertial term $\partial\psi/\partial t$ (see Greenspan & Howard (1963) for a full discussion).

2.3. Solution

The solution of (20)–(22) satisfying the conditions (23)–(25) and (27) may be expressed as a series of Bessel functions. A detailed discussion of the expansion, including completeness and termwise differentiation, is given in I, so we only quote the results here. The expansions are

$$T(r, z, t) = T_0(z, t) + \sum_{n=1}^{\infty} T_n(z, t) J_0(\gamma_n r), \tag{28}$$

$$V(r, z, t) = \sum_{n=1}^{\infty} V_n(z, t) J_1(\gamma_n r) \tag{29}$$

and
$$\psi(r, z, t) = \sum_{n=1}^{\infty} \psi_n(z, t) J_1(\gamma_n r), \tag{30}$$

where J_0 and J_1 are Bessel functions and γ_n is the n th positive root of $J_1 = 0$. Insertion of these expansions into (20)–(22) (see I for details) yields the following equations:

$$2\partial V_n/\partial z = -\gamma_n T_n, \tag{31}$$

$$\partial V_n/\partial t = -2\partial\psi_n/\partial z, \tag{32}$$

$$S^{-1} \partial T_0/\partial t = \partial^2 T_0/\partial z^2 \tag{33}$$

and
$$S^{-1} \partial T_n/\partial t = \gamma_n \psi_n + \partial^2 T_n/\partial z^2 - \gamma_n^2 T_n. \tag{34}$$

The boundary conditions (23) and (24) become

$$T_0 = T_n = 0 \quad \text{at} \quad z = 0 \tag{35}$$

and
$$2\lambda\psi_n + V_n = \rho_n, \tag{36}$$

where
$$r = \sum_{n=1}^{\infty} \rho_n J_1(\gamma_n r), \tag{37}$$

with
$$\rho_n = 2/\gamma_n J_2(\gamma_n). \tag{38}$$

The initial conditions (27) are now

$$T_0 = T_n = V_n = 0 \quad \text{at} \quad t = 0. \tag{39}$$

In addition, we require that the solution be well behaved as $z \rightarrow \infty$.

It is easy to show that $T_0 \equiv 0$. The rest of the solution is readily obtained by a Laplace transform in time. We denote the transforms by overbars and let p be the transform variable. Then one can show that

$$\bar{V}_n = A_n \left\{ \frac{\exp(-\alpha_n z)}{\alpha_n} - \frac{\exp(-\beta_n z)}{\beta_n} \right\}, \tag{40}$$

$$\bar{T}_n = (2A_n/\gamma_n) \{ \exp(-\alpha_n z) - \exp(-\beta_n z) \} \tag{41}$$

and
$$\bar{\psi}_n = \frac{pA_n}{2} \left\{ \frac{\exp(-\alpha_n z)}{\alpha_n^2} - \frac{\exp(-\beta_n z)}{\beta_n^2} \right\}, \tag{42}$$

where
$$A_n = \frac{\rho_n \alpha_n^2 \beta_n^2}{p(\beta_n - \alpha_n)(\alpha_n \beta_n + p\lambda[\alpha_n + \beta_n])} \tag{43}$$

and
$$\left\{ \begin{matrix} \alpha_n^2 \\ \beta_n^2 \end{matrix} \right\} = \frac{1}{2} \left(\frac{p}{S} + \gamma_n^2 \right) \mp \frac{1}{2} \left\{ \left(\frac{p}{S} + \gamma_n^2 \right)^2 - \gamma_n^2 p \right\}^{\frac{1}{2}}. \tag{44}$$

The evaluation of the solution is discussed in §4. There is one simple result which we present here, namely, an expression for the azimuthal velocity $V(1, z, t)$ on the side wall. Since this is derived in detail in I, we only quote the result here. The Laplace transform is

$$\bar{V}(1, z, p) = (p + 2\lambda p^{\frac{3}{2}})^{-1} \exp[-z(\frac{1}{4}p)^{\frac{1}{2}}]. \tag{45}$$

For $\lambda = 0$ (a case considered in detail later), the inversion is easily accomplished to give

$$V(1, z, t) = \operatorname{erfc}(z/4t^{\frac{1}{2}}). \tag{46}$$

3. Qualitative discussion of the flow

3.1. Layer structure

The principal features of the evolution of each radial harmonic are contained in (44). A description may be obtained in a straightforward way by identifying α_n and β_n as reciprocal vertical length scales and p as a reciprocal time. The correctness of the description so obtained will be verified in the more quantitative discussion of §4.

By examining the dependence of α_n^2 and β_n^2 on p , one finds three distinct time regimes: (i) $t \ll (\gamma_n S)^{-2}$ (corresponding to $p \gg (\gamma_n S)^2$), (ii) $(\gamma_n S)^{-2} \ll t \ll \gamma_n^{-2}$ (corresponding to $\gamma_n^2 \ll p \ll (\gamma_n S)^2$) and (iii) $t \gg \gamma_n^{-2}$ (corresponding to $p \ll \gamma_n^2$). We consider them in turn. For $t \ll (\gamma_n S)^{-2}$, we have

$$\alpha_n^2 \simeq \frac{1}{4} \gamma_n^2 S, \quad \beta_n^2 \simeq p/S.$$

Thus there is a horizontal layer of constant thickness $\alpha_n^{-1} = 2/(\gamma_n S^{\frac{1}{2}})$, which is the basic *RS* layer. The other layer has a time-dependent thickness

$$\beta_n^{-1} = (S/p)^{\frac{1}{2}} \sim (St)^{\frac{1}{2}}.$$

The dimensional thickness is $(\chi t^*)^{\frac{1}{2}}$, where t^* is dimensional time, and we see that the β layer is simply a thermal diffusion layer. For $t \ll (\gamma_n S)^{-2}$, the thermal layer is thinner than the *RS* layer. This time regime ends when the growing thermal layer reaches the *RS* layer, at a time $t \sim (\gamma_n S)^{-2}$. At this time, the layers actually merge to form a single, higher order layer. This result is established by considering the next time regime $(\gamma_n S)^{-2} \ll t \ll \gamma_n^{-2}$. In that range

$$\left\{ \begin{matrix} \alpha_n^2 \\ \beta_n^2 \end{matrix} \right\} \simeq \mp \frac{1}{2} i \gamma_n p^{\frac{1}{2}},$$

so that both vertical length scales are of order $(t/\gamma_n^2)^{\frac{1}{2}}$. Thus there is a single layer which diffuses inward according to a $t^{\frac{1}{2}}$ law. We shall call this flow regime the intermediate diffusion mode. As this regime ends ($t \sim \gamma_n^{-2}$), the layer splits again into two layers. This is seen by examining α_n^2 and β_n^2 for $t \gg \gamma_n^{-2}$. We find that

Time	Layer type and thickness	Dominant terms in thermal equation
$t^* \ll \frac{\delta_n^{*2}}{\chi}$	Thermal diffusion layer $\sim (\chi t^*)^{\frac{1}{2}}$ Rotational shear layer for n th harmonic $\sim \delta_n^*$	$S^{-1}(\partial T_n / \partial t) = (\partial^2 T_n / \partial z^2)$ $S^{-1}(\partial T_n / \partial t) = \gamma_n \psi_n$
$t^* \sim \frac{\delta_n^{*2}}{\chi}$	Thermal and rotational shear layers merge $\sim \delta_n^*$	$S^{-1}(\partial T_n / \partial t) = \gamma_n \psi_n + (\partial^2 T_n / \partial z^2)$
$\frac{\delta_n^{*2}}{\chi} \ll t^* \ll t_n^*$	Intermediate diffusion layer $\sim (R/\gamma_n)(t^*/t_n^*)^{\frac{1}{2}}$	$0 = \gamma_n \psi_n + (\partial^2 T_n / \partial z^2)$
$t^* \sim t_n^*$	Intermediate diffusion layer bifurcates $\sim (R/\gamma_n)$	$0 = \gamma_n \psi_n + (\partial^2 T_n / \partial z^2) - \gamma_n^2 T_n$
$t^* \gg t_n^*$	Harmonic layer $\sim (R/\gamma_n)$ Final diffusion layer $\sim R(t^*/t_{ES}^*)^{\frac{1}{2}}$	$0 = (\partial^2 T_n / \partial z^2) - \gamma_n^2 T_n$ $0 = \gamma_n \psi_n - \gamma_n^2 T_n$

TABLE 1. Qualitative layer structure of interior flow as a function of time t^* . The thickness of the rotational shear layer for the n th radial harmonic is δ_n^* , R is the radius of the cylinder, χ is the thermal diffusivity, γ_n is the n th root of $J_1 = 0$, $t_{ES}^* = SR^2/\chi$ is the Eddington-Sweet time based on the radius and $t_n^* = SR^2/(\chi\gamma_n^2)$ is a kind of Eddington-Sweet time for the n th harmonic. The last column shows the dominant terms in the (dimensionless) thermal equation (34).

$\alpha_n^2 \simeq \frac{1}{4}p$ and $\beta_n^2 \simeq \gamma_n^2$. Thus there is a stationary layer of thickness $\beta_n^{-1} \simeq \gamma_n^{-1}$ and a growing layer of thickness $\alpha_n^{-1} \sim 2t^{\frac{1}{2}}$. The stationary layer corresponds to a harmonic function in the temperature field. Such a function would be required by more general thermal boundary conditions than those considered in the present work. The other mode is a kind of diffusion mode which continues to propagate inward. We call this last mode the final diffusion mode. These considerations are summarized in table 1. In that table, t^* is the dimensional time, $t_{ES}^* = SR^2/\chi$ is the Eddington-Sweet time based on the radius, $t_n^* = SR^2/(\chi\gamma_n^2)$ is a kind of Eddington-Sweet time based on the radial scale of the n th harmonic, and $\delta_n^* = R/(\gamma_n S^{\frac{1}{2}})$ is the thickness of the RS layer for the n th radial harmonic. Each radial harmonic has its own length and time scale. Thus the higher harmonics go through the sequence of states more rapidly. Nevertheless, the final penetration occurs on the same time scale for all of the radial modes: the penetration law for the final diffusion layer is independent of n . This result is consistent with the quantitative results of I for a cylinder of finite height.

The various flow regimes in table 1 may be characterized by the relative order of terms in the thermal equation (34). It is not hard to make such estimates, and the last column in the table gives the dominant terms in the equation. Although the flow is driven by thermal diffusion, the time scale differs from L^2/χ (where L is the length scale) because of constraints imposed by mechanical equilibrium. Equation (20) shows that any change in the radial structure of the temperature field requires a change in the azimuthal velocity field. From (21), it follows that such changes require circulations. Thus the thermal diffusion and motions are inextricably linked. The magnitude of the circulations is governed by the thermal equation (22), and the different regimes in table 1 correspond to dominance of different terms in the equation.

3.2. Ekman pumping and the parameter λ

The discussion so far, based entirely on α_n and β_n , takes no account of the boundary conditions. The amplitudes of the various layers depend on the boundary conditions, in particular on the parameter λ . The fact that $\lambda \ll 1$ suggests the possibility of the significant simplification $\lambda = 0$. The analysis in this section shows that, for most purposes, we can take $\lambda = 0$ provided that $\lambda S^{\frac{1}{2}} \ll 1$. Since $S \gg 1$ (by assumption), this provides a definite criterion of smallness for λ .

We begin by examining the solution (40)–(44) for the case $\lambda = 0$. One can show, after some calculation, that $\lim_{t \rightarrow 0} V \neq 0$, in spite of the initial condition

$V = 0$ at $t = 0$. Thus there is some instantaneous spin-up for $\lambda = 0$. This is to be expected, since $\lambda \rightarrow 0$ corresponds to the Ekman time approaching zero. In fact detailed calculations show the following: the limit as $t \rightarrow 0$ of the solution for $\lambda = 0$ is equal to the limit as $t \rightarrow \infty$ of the adiabatic spin-up solutions of Sakurai (1969) and Walin (1969). Thus for λ sufficiently small, we get first adiabatic spin-up, followed by a thermal relaxation of the adiabatic spin-up state. From this picture, we can calculate how small λ must be; for the correctness of the picture requires that the adiabatic spin-up time t_{RS} for the RS layer be much smaller than the time scale δ_{RS}^2/χ for thermal effects to penetrate the RS layer. From Walin (1969) and Sakurai (1969) we have (in dimensional form) $t_{RS} = S^{-\frac{1}{2}}t_{EK}$, hence we require

$$S^{-\frac{1}{2}}t_{EK} \ll \delta_{RS}^2/\chi,$$

or

$$\lambda S^{\frac{1}{2}} \ll 1. \tag{47}$$

If, on the other hand, $\lambda S^{\frac{1}{2}} \gg 1$, thermal effects dominate the RS layer from the outset. In the remainder of the present work, we assume that (47) holds. Then we may legitimately take $\lambda = 0$, as long as we have no need to resolve the initial, rapid, adiabatic spin-up of the RS layer.

The conclusions which have been sketched here can be obtained more formally by rescaling the equations in a way suggested by the results of Walin (1969) and Sakurai (1969), and then studying the limit $S \rightarrow \infty$, $\lambda \rightarrow 0$ with $\lambda S^{\frac{1}{2}} \rightarrow 0$. The analysis is somewhat lengthy so we do not give it here. It is perhaps worth noting that an analysis of each radial harmonic replaces (47) with $\lambda S^{\frac{1}{2}}\gamma_n \ll 1$, and we require this to be satisfied for all important harmonics.

4. Quantitative results for impulsive spin-up

4.1. Preliminary simplifications

The computational problem is the determination of the coefficients V_n , ψ_n and T_n , and the subsequent summation of the series (28)–(30). In earlier work on stratified spin-up, the series were poorly converging. The present work is no exception, and many terms are needed to represent the solution with reasonable accuracy. Fortunately, the coefficients for different values of n are related by

a simple similarity transformation, so that it is only necessary to evaluate three functions rather than a triple infinity of functions. We write the expansions (28)–(30) as follows:

$$T(r, z, t) = \sum_{n=1}^{\infty} \rho_n R(\gamma_n z, \gamma_n^2 t) J_0(\gamma_n r), \tag{48}$$

$$V(r, z, t) = \sum_{n=1}^{\infty} \rho_n W(\gamma_n z, \gamma_n^2 t) J_1(\gamma_n r), \tag{49}$$

$$\psi(r, z, t) = \sum_{n=1}^{\infty} \gamma_n \rho_n \Phi(\gamma_n z, \gamma_n^2 t) J_1(\gamma_n r). \tag{50}$$

As the notation indicates, the functional form of R , W and Φ is independent of n . Thus $R(\xi, \tau)$, $W(\xi, \tau)$ and $\Phi(\xi, \tau)$ are solutions of

$$2\partial W/\partial \xi = -R, \tag{51}$$

$$\partial W/\partial \tau = -2\partial \Phi/\partial \xi \tag{52}$$

and

$$S^{-1} \partial R/\partial \tau = \partial^2 R/\partial \xi^2 - R + \Phi, \tag{53}$$

with

$$W = R = 0 \quad \text{for} \quad \tau = 0 \tag{54}$$

and

$$R = W - 1 = 0 \quad \text{for} \quad \xi = 0. \tag{55}$$

In addition, W , R and Φ should vanish as $\xi \rightarrow \infty$. In the formulation, we have taken $\lambda = 0$, in accordance with the discussion of §3.2. The problem (51)–(55) is solved by Laplace transforms. We let p be the transform variable. Then the transforms \bar{W} , \bar{R} and $\bar{\Phi}$ are given by

$$\bar{W} = \frac{\beta e^{-\alpha z} - \alpha e^{-\beta z}}{p(\beta - \alpha)}, \tag{56}$$

$$\bar{R} = \frac{2\alpha\beta(e^{-\alpha z} - e^{-\beta z})}{p(\beta - \alpha)} \tag{57}$$

and

$$\bar{\Phi} = \frac{\beta^2 e^{-\alpha z} - \alpha^2 e^{-\beta z}}{2\alpha\beta(\beta - \alpha)}, \tag{58}$$

where

$$\left\{ \begin{matrix} \alpha^2 \\ \beta^2 \end{matrix} \right\} = \frac{1}{2} \left(1 + \frac{p}{S} \right) \mp \frac{1}{2} \left\{ \left(1 + \frac{p}{S} \right)^2 - p \right\}^{\frac{1}{2}}. \tag{59}$$

In performing the inversions, we note that the only singularities of the transforms are a pole at $p = 0$ and branch points at $p = 0, \infty$, which we connect by a branch cut along the negative real axis. By deforming the inversion contour around the branch cut, we get the following result for $W(\xi, \tau)$:

$$W(\xi, \tau) = 1 + \int_0^{\infty} dv (\pi Q)^{-1} \exp(-v^2 \tau) [\cos(A\xi) - e^{-B\xi} - (B/A) \sin(A\xi)], \tag{60}$$

where

$$\left\{ \begin{matrix} A \\ B \end{matrix} \right\} = \left\{ \frac{Q}{2} \mp \frac{1}{2} \left(1 - \frac{v^2}{S} \right) \right\}^{\frac{1}{2}}, \tag{61}$$

with

$$Q = \{v^2 + (1 - v^2/S)^2\}^{\frac{1}{2}}. \tag{62}$$

Similar expressions may be derived for R and Φ . In what follows, however, we concentrate completely on W , as it is the quantity of greatest interest. The integration in (60), and the summation of the series (49), must be done numerically. Fortunately, a further simplification is possible. We can exploit the fact that $S \gg 1$ and develop asymptotic expressions for the limit $S \rightarrow \infty$. This reduces the solution from a function of four variables (r, z, t, S) to one of three (r, z, t). The approximation is not uniformly valid in time but, as the calculations show, two distinct limits suffice to cover the whole time range. In §4.2, we consider the long-time limit, obtained by taking $S \rightarrow \infty$ at fixed ξ and τ . This limit is adequate for the description of the intermediate and final diffusion modes, but it misses the earlier merging of the RS and thermal layers, which occurs for $\tau = O(S^{-2})$. In §4.3, we rescale ξ and τ , by letting $\eta = S^{\frac{1}{2}}\xi$ and $\sigma = S^2\tau$. The limit $S \rightarrow \infty$ at fixed η and σ then gives a useful short-time approximation. The overlap of these two limits is established below.

4.2. Intermediate diffusion mode

We let $S \rightarrow \infty$ at fixed r, z and τ . This is equivalent to dropping the thermal inertia term ($\partial R/\partial \tau$ in (53)) and dropping the thermal initial condition (on R). It follows directly from (60) that

$$\lim_{S \rightarrow \infty} W(\xi, \tau, S) = \tilde{W}(\xi, \tau) = 1 + \int_0^\infty dv (\pi q)^{-1} \exp(-v^2 \tau) \times [\cos(a\xi) - e^{-b\xi} - (b/a) \sin(a\xi)], \quad (63)$$

where
$$\begin{pmatrix} a \\ b \end{pmatrix} = \left\{ \frac{q \mp 1}{2} \right\}^{\frac{1}{2}}, \quad q = (v^2 + 1)^{\frac{1}{2}}.$$

The integral (63) has been evaluated numerically for $0.01 \leq \tau \leq 100$ and $0 \leq \xi \leq 100$. In summing the series (49), it is necessary, because of poor convergence, to have values of \tilde{W} for large ξ and τ , that is, we need $\tilde{W}(\gamma_n z, \gamma_n^2 t)$ for large γ_n . We get these values by an asymptotic expansion of \tilde{W} for $\tau \rightarrow \infty$ with $\zeta = \xi/2\tau^{\frac{1}{2}}$ fixed (for $\xi = \gamma_n z$ and $\tau = \gamma_n^2 t$, we have $\zeta = z/2t^{\frac{1}{2}}$). Such an expansion is obtained by lengthy but straightforward calculations from (63), and the result is

$$\tilde{W}(\xi, \tau) = \operatorname{erfc}(\frac{1}{2}\zeta) + \frac{\exp(-\frac{1}{4}\zeta^2)}{(4\pi\tau)^{\frac{1}{2}}} + \frac{\zeta(6 - \zeta^2)\exp(-\frac{1}{4}\zeta^2)}{32\tau\pi^{\frac{1}{2}}} + E, \quad (64)$$

where
$$E = \frac{(-16 + 14\zeta^2 - \zeta^4)\exp(-\frac{1}{4}\zeta^2)}{128(\pi\tau^3)^{\frac{1}{2}}} + O(\tau^{-2}). \quad (65)$$

With \tilde{W} replaced by the expansion (64), the series (49) becomes

$$\begin{aligned} \tilde{V}(r, z, t) = & r \operatorname{erfc}(\frac{1}{2}\zeta) + \frac{G(r)\exp(-\frac{1}{4}\zeta^2)}{(4\pi t)^{\frac{1}{2}}} \\ & + \frac{H(r)\zeta(6 - \zeta^2)\exp(-\frac{1}{4}\zeta^2)}{32t\pi^{\frac{1}{2}}} + \sum_{n=1}^\infty \rho_n E_n J_1(\gamma_n r), \end{aligned} \quad (66)$$

where we have used (37), where $\zeta = z/(2t^{\frac{1}{2}})$ and where

$$G(r) = \sum_{n=1}^{\infty} \rho_n \gamma_n^{-1} J_1(\gamma_n r), \quad H(r) = \sum_{n=1}^{\infty} \rho_n \gamma_n^{-2} J_1(\gamma_n r) \tag{67}$$

and

$$E_n = E(\gamma_n z, \gamma_n^2 t). \tag{68}$$

The series for G and H can be summed numerically. They are alternating series with terms of magnitude n^{-2} for G and n^{-3} for H . The coefficient E_n is calculated, for $\gamma_n^2 t \leq 100$, from (64) with numerical integration for \tilde{W} . For $\gamma_n^2 t > 100$, E_n is calculated from (65) by dropping the $O(\tau^{-2})$ term. The series in (66) is then summed numerically. Since $\rho_n E_n J_1 = O(n^{-4})$, there are no real difficulties with convergence.

As $r \rightarrow 0$, convergence becomes worse than the above estimates would indicate. This can be seen from the formula for $r = 0$. If $\tilde{\Omega} = \tilde{V}/r$, then it follows from (66) that

$$\begin{aligned} \tilde{\Omega}(0, z, t) = \operatorname{erfc} \left(\frac{1}{2} \zeta \right) + \frac{\exp \left(-\frac{1}{4} \zeta^2 \right)}{4(\pi t)^{\frac{1}{2}}} \left(\sum_{n=1}^{\infty} \rho_n \right) \\ + \frac{\zeta(6 - \zeta^2) \exp \left(-\frac{1}{4} \zeta^2 \right)}{64t\pi^{\frac{1}{2}}} \left(\sum_{n=1}^{\infty} \frac{\rho_n}{\gamma_n} \right) + \frac{1}{2} \sum_{n=1}^{\infty} \rho_n \gamma_n E_n. \end{aligned} \tag{69}$$

The convergence is not as good, since $\rho_n \gamma_n E_n = O(n^{-\frac{5}{2}})$.

For $r \rightarrow 1$, we may make use of the exact result (46) to get

$$\tilde{V}(1, z, t) = \operatorname{erfc} \left(\frac{1}{2} \zeta \right), \tag{70}$$

an explicit formula for the velocity on the side wall.

These formulae have been used to compute $\tilde{\Omega}$ for various values of r , z and t . The values were all computed as described above, except for the small range $0 \leq r \leq 0.05$, in which extrapolation was used. The principal features of the solution can be seen in figure 1, which shows $\tilde{\Omega}$ as a function of r , for four values of z at each of four times. For the smallest time ($t = 0.01$), there is much greater spin-up near the centre than at the side walls. Spin-up on the side walls requires boundary-layer suction into the side-wall layer, and this takes time to develop, because density diffusion is required to break the constraint of buoyancy forces on the material in the side-wall layer. The Ekman suction, on the other hand, begins immediately. Thus the side-wall spin-up lags behind the axial spin-up. The resulting adverse gradient of angular momentum strongly suggests the likelihood of a rotational instability, a somewhat unexpected result for spin-up. For somewhat larger times ($t = 0.1$), the spin-up has penetrated further in the z direction, and the radial profiles are somewhat flatter. For $t = 1.0$, the profiles are fairly flat and for $t = 10.0$, the profiles are within 3% or less of being perfectly flat. This is consistent with the analysis, since it follows from (66) that

$$\tilde{\Omega} \rightarrow \operatorname{erfc} \left(\frac{1}{2} \zeta \right)$$

as $t \rightarrow \infty$ (at fixed ζ). The numerical results show that this asymptotic state (called the final diffusion layer in §3) is reached for $t \gtrsim 1$.

To compare the present results with the small-time limit of §4.3, we need an asymptotic formula for small τ . For $\tau \ll 1$, the integral (63) may be approximated

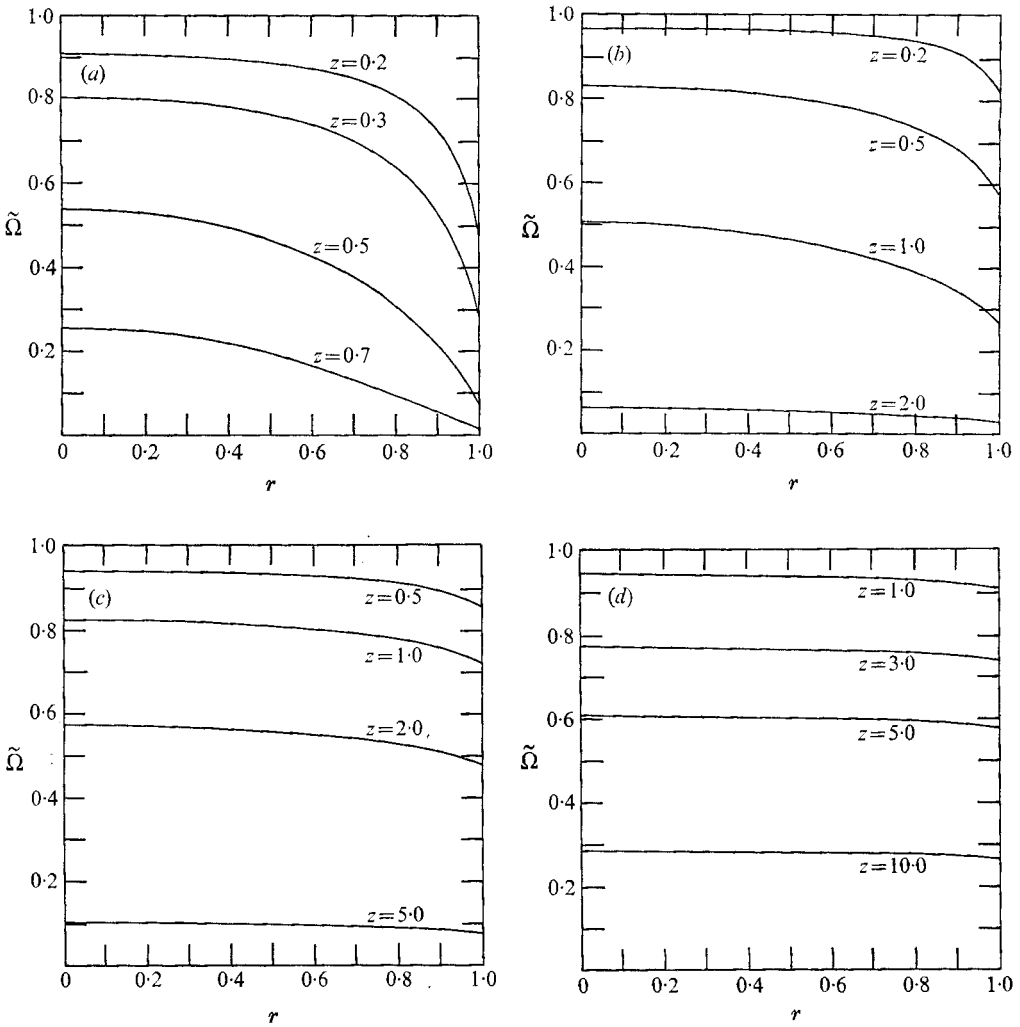


FIGURE 1. Angular velocity $\tilde{\Omega}$ in the long-time limit as a function of radius r for selected values of height z at (a) $t = 0.01$, (b) $t = 0.1$, (c) $t = 1.0$ and (d) $t = 10.0$. The unit of time is the Eddington-Sweet time and the unit of height is the cylinder radius.

by observing that the large values of v are important, so that we can take $q \simeq v$, $a \simeq b \simeq (\frac{1}{2}v)^{\frac{1}{2}}$. Then we get

$$\tilde{W} \underset{\tau \rightarrow 0}{\sim} F(\lambda) = 1 + \int_0^\infty du (2\pi u)^{-1} e^{-u} [\cos(\lambda u^{\frac{1}{2}}) - \exp(-\lambda u^{\frac{1}{2}}) - \sin(\lambda u^{\frac{1}{2}})], \quad (71)$$

where $\lambda = \xi/(4\tau)^{\frac{1}{2}}$ is the natural similarity parameter for small times. Thus $\tilde{W}(\gamma_n z, \gamma_n^2 t)$ is asymptotic to $F(\lambda)$ with $\lambda = \gamma_n z / (4\gamma_n^2 t)^{\frac{1}{2}} = z(\gamma_n^2/t)^{\frac{1}{2}}$.

4.3. *Merging of thermal and RS layers*

The proper length and time scaling for this flow regime are determined by the thickness $S^{-\frac{1}{2}}$ of the *RS* layer and the time S^{-2} at which the layers merge. Thus we introduce

$$y = S^{\frac{1}{2}}z, \quad T = S^2t. \tag{72}$$

From (49) we have

$$V = \sum_{n=1}^{\infty} \rho_n W(\gamma_n S^{-\frac{1}{2}}y, \gamma_n^2 S^{-2}T) J_1(\gamma_n r). \tag{73}$$

We abbreviate $\gamma_n y$ by η and $\gamma_n^2 T$ by σ . Then from (60)–(62) we get

$$\lim_{S \rightarrow \infty} W(S^{-\frac{1}{2}}\eta, S^{-2}\sigma) = \hat{W}(\eta, \sigma) = 1 + \int_0^{\infty} \frac{dv \exp(-\sigma v^2)}{\pi(v^2 + v^4)^{\frac{1}{2}}} \times \left\{ \cos(\hat{A}\eta) - \exp(-\hat{B}\eta) - \left(\frac{\hat{B}}{\hat{A}}\right) \sin(\hat{A}\eta) \right\}, \tag{74}$$

where $\left(\frac{\hat{A}}{\hat{B}}\right) = \left\{ \frac{1}{2} [\pm v^2 + (v^4 + v^2)^{\frac{1}{2}}] \right\}^{\frac{1}{2}}$.

In this limit,

$$V = \hat{V}(y, T) = \sum_{n=1}^{\infty} \rho_n \hat{W}(\gamma_n y, \gamma_n^2 T) J_1(\gamma_n r). \tag{75}$$

The connexion with the formulae of §4.2 is easily made. It is not difficult to show from (74) that

$$\hat{W}(\eta, \sigma) \sim F(\mu), \quad \text{as } \sigma \rightarrow \infty,$$

where F is defined by (71), and $\mu = \eta/(4\sigma)^{\frac{1}{2}}$. Then $\hat{W}(\gamma_n y, \gamma_n^2 T)$ is asymptotic to $F(\mu)$ with

$$\mu = \gamma_n y / (4\gamma_n^2 T)^{\frac{1}{2}} = z(\gamma_n^2/t)^{\frac{1}{2}}.$$

Thus the long-time limit of the present (short-time) solution agrees with the short-time limit of the previous (long-time) solution, and this ensures that the two different $S \rightarrow \infty$ limits cover the entire range.

Values of \hat{W} are obtained from (74) by numerical integration. For large values of σ , it is more convenient to work with the form

$$\hat{W}(\eta, \sigma) = 1 + \frac{2}{\pi} \int_0^{\infty} \frac{dv \exp[-v^2/(1 + \epsilon v^2)]}{v(1 + \epsilon v^2)^{\frac{1}{2}}} \left\{ \cos(\kappa v) - \frac{\sin(\kappa v)}{(1 + \epsilon v^2)^{\frac{1}{2}}} - \exp\left[-\frac{\kappa v}{(1 + \epsilon v^2)^{\frac{1}{2}}}\right] \right\}, \tag{76}$$

where $\epsilon = 2/\sigma^{\frac{1}{2}}$ and $\kappa = \eta/(4\sigma)^{\frac{1}{2}}$. The summing of the series requires $\hat{W}(\gamma_n y, \gamma_n^2 T)$, and since the convergence is poor, we need the values for large n . Although analytical asymptotic formulae can be developed for $\hat{W}(\eta, \sigma)$ as $\sigma \rightarrow \infty$ with η^2/σ fixed, it turns out to be more accurate and convenient simply to evaluate (76) numerically. Even for $\sigma = 10^6$ there are no difficulties with the integration. Thus the computational basis for determining $\hat{V}(y, T)$ is (74)–(76).

There is one complication with the small-time limit considered here, and that is the fact that different radial harmonics evolve at different rates. For large n , the argument $\sigma = \gamma_n^2 T$ of \hat{W} can become so large that the small-time limit is

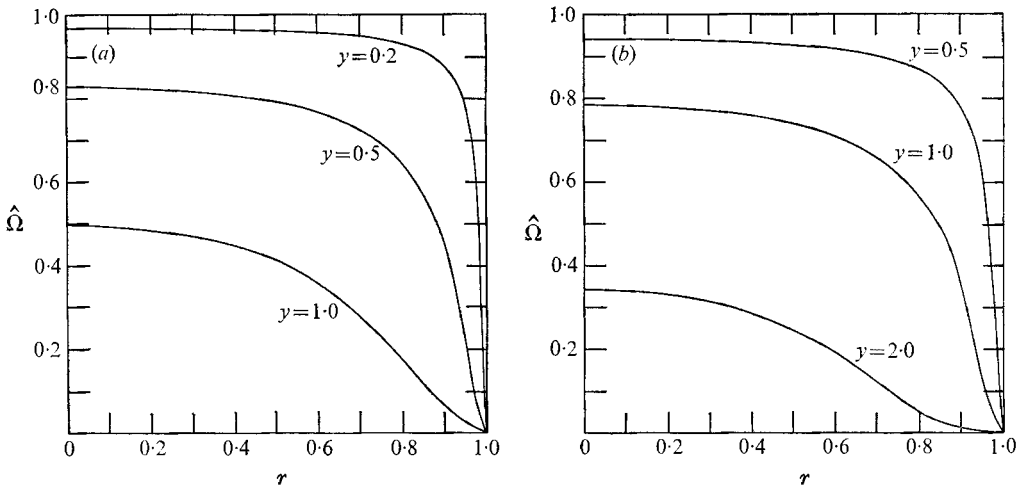


FIGURE 2. Angular velocity $\hat{\Omega}$ in the short-time limit as a function of radius r for selected values of height y at (a) $T = 0.1$ and (b) $T = 1.0$. The unit of time is t_M , the time at which the thermal layer and the rotational shear layer merge. The unit of height y is the thickness of the rotational shear layer.

no longer valid. In order to use the series (75) without modification, T must be sufficiently small that $\gamma_n^2 T$ remains in the small-time range for all important radial harmonics. Another way to state the constraint is that, for any given T , S must be sufficiently large (making S larger increases the small-time range).

Because of this, we have carried out calculations of \hat{V} only for moderate values of T . The results are shown in figure 2, which gives $\hat{\Omega}$ as a function of r for various values of y , for $T = 0.1$ and 1.0 . The adverse angular momentum gradients near the side wall are even more pronounced here than in the long-time limit. As one can show from (46), there is no spin-up on the side wall in the short-time limit.

Some insight into the nature of the two layers may be obtained from further analysis. We start with the representation (74) for $\hat{W}(\eta, 0)$. One can show that

$$\hat{W}(\eta, 0) = 1 + \int_0^\infty \frac{dv}{\pi(v^2 + v^4)^{\frac{1}{2}}} \{ \cos(\hat{A}\eta) - \exp(-\hat{B}\eta) - (\hat{B}/\hat{A}) \sin(\hat{A}\eta) \} = e^{-\frac{1}{2}\eta}, \tag{77}$$

a result which is most easily established from the Laplace transform of the solution. This is just the instantaneous spin-up of the RS layer. By combining (77) and (74), we get

$$\hat{W}(\eta, \sigma) = \hat{W}_{RS}(\eta, \sigma) + \hat{W}_T(\eta, \sigma), \tag{78}$$

where
$$\hat{W}_{RS} = e^{-\frac{1}{2}\eta} + \int_0^\infty \frac{dv [1 - \exp(-v^2\sigma)]}{\pi(v^4 + v^2)^{\frac{1}{2}}} \exp(-\hat{B}\eta) \tag{79}$$

is the RS -layer portion of the solution and

$$\hat{W}_T = \int_0^\infty \frac{dv [1 - \exp(-v^2\sigma)]}{\pi v (1 + v^2)^{\frac{1}{2}}} \left\{ \frac{\hat{B}}{\hat{A}} \sin(\hat{A}\eta) - \cos(\hat{A}\eta) \right\} \tag{80}$$

is the thermal-layer portion. The distinction is meaningful only before the two layers have merged, that is, for small σ . For small σ , we may use the approxima-

tions $\hat{A} \simeq v$, $\hat{B} \simeq \frac{1}{2}$ and $(1 + v^2)^{\frac{1}{2}} \simeq v$. The resulting integrals can be evaluated, and we get

$$\hat{W}_{RS}(\eta, \sigma) \simeq [1 + (\sigma/\pi)^{\frac{1}{2}}] e^{-\frac{1}{2}\eta} \tag{81}$$

and

$$\hat{W}_T(\eta, \sigma) \simeq \frac{1}{4}\sigma \operatorname{erf}(\eta/2\sigma^{\frac{1}{2}}) + \eta(\eta - 4)(16\pi^{\frac{1}{2}})^{-1} E_{\frac{3}{2}}(\eta^2/4\sigma), \tag{82}$$

where

$$E_{\frac{3}{2}}(z) = \int_z^\infty dv v^{-\frac{3}{2}} e^{-v}$$

is the exponential integral of order $\frac{3}{2}$. The principal result from these formulae is that $|\hat{W}_T| \ll |\hat{W}_{RS}|$ in this regime. (For example, $\hat{W}_{RS}(0, \sigma) = 1 + (\sigma/\pi)^{\frac{1}{2}}$, whereas $-\hat{W}_T(0, \sigma) = \sigma/\pi^{\frac{1}{2}} \ll 1$.) Thus before the layers merge, the angular velocity increment is carried by the *RS* layer.

5. Summary of time scales

We give here a qualitative summary of the various time scales and the role they play in spin-up. We do not consider the individual radial harmonics, so the discussion is less accurate than that in §3.1. We consider the time scales in order of increasing size, and the discussion presumes the ordering of time scales given in §1. We use dimensional quantities throughout this section.

The smallest time scale is the rotation period Ω^{-1} . This is the time it takes the Ekman layer to form, after the impulsive spin-up of the boundary. The Ekman pumping begins to create an *RS* (rotational shear) layer of thickness $\delta_{RS} = RS^{-\frac{1}{2}}$. The (non-uniform) spin-up of the *RS* layer is complete in a time

$$t_{RS} = \Omega^{-1} S^{-\frac{1}{2}} E^{-\frac{1}{2}} = (\delta_{RS}^2/\nu\Omega)^{\frac{1}{2}}$$

For times greatly exceeding t_{RS} , the drop in Ω across the Ekman layer is very small, and may be ignored (that is, we may take $\lambda = 0$ in the boundary condition (23)). Meanwhile, a thermal layer, of thickness δ_T , generated at the wall, is diffusing outwards according to the law $\delta_T = (\chi t)^{\frac{1}{2}}$. This layer merges with the *RS* layer at a time $t_M = \delta_{RS}^2/\chi$. During the time range $t_{RS} < t < t_M$, the angular velocity is quasi-steady, and the total applied increment $\Delta\Omega$ in angular velocity occurs across the *RS* layer. After the layers merge, the angular velocity diffuses inwards in what we have called the intermediate diffusion mode. In this regime ($t > t_M$), the angular velocity increment $\Delta\Omega$ is distributed over a layer of thickness $\delta_I = R(t/t_{RS})^{\frac{1}{2}}$, where $t_{ES} = SR^2/\chi$ is the Eddington–Sweet time. For a cylinder of aspect ratio near unity, or for a sphere, the spin-up process is essentially over for $t \sim t_{ES}$. For a cylinder with height $H \gg R$, the process continues in what we have called the final diffusion mode, which reaches the centre at a time SH^2/χ .

It is worth noting that the thermal diffusion (Kelvin–Helmholtz) time scale $t_{KH} = R^2/\chi$ does not play an important role in the spin-up process. As is shown by (33), the average temperature $T_0(z, t)$ on equipotentials adjusts on this time scale. No buoyancy forces are associated with variations in T_0 , so such adjustments play no role in spin-up.

The case of continuous spin-up adds another time scale, namely the time scale t_B on which the boundary velocity is changed. The character of the resulting

spin-up depends on where t_B fits into the hierarchy of internal time scales. Those internal processes with scales comparable with or larger than t_B will determine the distribution of angular velocity. If, for example, $t_M \ll t_B \ll t_{ES}$, then the complicated description of the thermal layer, the *RS* layer and their merging is unnecessary. The angular velocity distribution can be calculated by using only the large-time solution of §4.2. Thus if $\Omega_B(t)$ is the boundary value of the increment in Ω , then for $t_B \gg t_M$ we have

$$V(r, z, t) = \int_0^t dt' \bar{V}(r, z, t-t') \Omega_B(t'). \quad (83)$$

An important quantity which depends on the time scales is the gradient of angular velocity. For impulsive spin-up, the maximum gradient is $\Delta\Omega/\delta_{RS}$, where $\Delta\Omega$ is the boundary increment. This gradient persists until $t > t_M$. The same is true for continuous spin-up if $t_B \ll t_M$. If, however, $t_B > t_M$, but $t_B < t_{ES}$, then an estimate of the gradient is $\Delta\Omega/\delta_I = (\Delta\Omega/R)(t_B/t_{ES})^{\frac{1}{2}}$. Finally, for $t_B \gg t_{ES}$, the gradient is comparable with $(\Delta\Omega/R)(t_{ES}/t_B)$.

6. Solar spin-down problem

The suggestion by Dicke (1964) that the interior of the sun rotates more rapidly than the visible surface layers has generated considerable interest in spin-down under solar conditions. The basic picture is the following. The magnetic solar wind exerts a non-negligible torque on the sun. The effects of the torque are distributed rapidly throughout the outer, turbulent convection zone. The question which bears directly on the Dicke hypothesis is that of the efficiency of angular momentum transport in the inner, convectively stable portion of the sun. Transport processes which take much longer than the age of the sun (5×10^9 yr) are not of interest. As Dicke (1964) and others have pointed out, viscous diffusion falls into this category, since the time scale is about 10^{13} yr.

The possible importance of the Ekman spin-down process was first suggested by Howard, Moore & Spiegel (1967). It is generally agreed that the interface between the interior and the convection zone should behave in some sense like an Ekman layer. As pointed out by Howard *et al.* (1967), the coupling between the two regions is greatly enhanced by entrainment. Bretherton & Spiegel (1968) have attempted to account for the entrainment by treating the convection zone as a porous solid. Their analysis shows that, in such a model, the pumping is very efficient; in fact, they find a characteristic spin-down time of the order of days. Clark, Thomas & Clark (1969) have accounted for entrainment in a somewhat different way. They point out that the transfer of angular momentum between the convection zone and the interior occurs mostly in the layer of penetrative convection separating these regions. This region of mixing then acts like an Ekman layer. Its thickness δ_{EK} , however, is determined entirely by the properties of the convection, and not by the rotation rate. On the basis of Roxburgh's (1965) work, the thickness may be estimated as $\delta_{EK} = 500$ km. The corresponding spin-down time is $L/\Omega\delta_{EK}$, which for $L = 5 \times 10^{10}$ cm (the inner radius of the convection zone) and $\Omega = 5.7 \times 10^{-5} \text{ s}^{-1}$ (the value suggested by Dicke) is of

the order of 6 months. The spin-down times t_{RS} for the rotational shear layer are even shorter. The Bretherton–Spiegel picture gives a time of a few hours; the penetrative convection picture gives t_{RS} of the order of a week. Although the time scales given by the two pictures differ somewhat, they are equivalent in the sense that both are much smaller than any time scales relevant in the interior dynamics. We consider next what these short Ekman spin-down times actually mean.

The Ekman time scale is simply a measure of the length of time over which an appreciable lag in angular velocity can persist across the Ekman layer. Alternatively, we may regard the Ekman layer as a pump, and the Ekman time scale as a measure of the internal impedance of the pump. Whether or not we get spin-down on the Ekman time scale depends entirely on the nature of the interior fluid, or in terms of the analogy, the spin-down time will depend on the impedance of the interior ‘load’ on the pump, as well as the pump impedance. In the present case, the interior impedance is dominant, since the interior time scales (t_M, t_{ES} , etc.) are all so very much longer than the Ekman time scale. In addition, the boundary time scale t_B is surely much greater than the Ekman time scale. In this situation, the Ekman pumping is so efficient that no $\Delta\Omega$ can be built up across the Ekman layer, and the parameter λ in the boundary condition (23) may be set to zero. The resulting Ekman circulations are far smaller than the maximum possible Ekman currents, and their magnitude is determined by t_B and the interior dynamics. This is in great contrast to the case of the impulsive spin-up of an unstratified fluid, in which the dominant impedance is the Ekman layer itself, with the result that the Ekman time scale is the spin-up time.

On the basis of the above picture, we summarize the procedure to be followed in performing a solar spin-down calculation. There is a single field of meridional circulations which is driven throughout the volume by thermal imbalances associated with the centrifugal force and at the boundary by Ekman pumping. The equations governing these circulations are the usual equations of the Eddington–Sweet theory (see, for example, Mestel 1965), plus the spin-down equation which relates the local change in Ω to the meridional circulations. At the boundary, there are several boundary conditions on the interior flow: a thermal boundary condition, and a no-slip condition on Ω . No conditions are imposed on the meridional circulations at the boundary. It is to be emphasized that the solution in no way depends on the Ekman time scale, provided only that the Ekman scale is much shorter than the relevant interior and boundary time scales.

Apart from possible instabilities, the time scale for spin-down, determined by the interior dynamics, is the Eddington–Sweet time scale (Howard, Moore & Spiegel 1967; Sakurai *et al.* 1971). If the interior of the sun is rotating as rapidly as Dicke suggests, then this time scale is comparable with the age of the sun. Several authors have proposed instabilities which might greatly shorten the time for spin-down. Goldreich & Schubert (1967), for example, have demonstrated the existence of a Rayleigh instability, in which the stabilizing effect of stratification is expunged by thermal relaxation for disturbances of sufficiently small scale. This instability and its consequences have been much discussed (see Dicke 1970;

Fricke & Kippenhahn 1972 for reviews) but its importance for the sun is still uncertain.

Howard *et al.* (1967) have conjectured that the rotational shear layer becomes unstable. Spiegel (1972) has discussed the possible consequences in some detail, and he suggests that spin-down may occur through a sequence of such instabilities, each one extending the zone of turbulence inward by the thickness of an RS layer. Let us consider this conjecture in the light of the present work. The RS layer, of thickness $\delta_{RS} = RS^{-\frac{1}{2}}$, has a lifetime of order $t_M = \delta_{RS}^2/\chi$. From Weyman's solar model as tabulated by Schwarzschild (1958, p. 259), we get the following estimates of parameters near but below the inner boundary of the convection zone:

$$\chi = 3.5 \times 10^7 \text{ cm}^2/\text{s}, \quad N = 1.5 \times 10^{-3} \text{ s}^{-1}, \quad S = (N/\Omega)^2 = 700, \quad R = 5 \times 10^{10} \text{ cm}$$

(inner radius of the convection zone), hence $\delta_{RS} = 1.9 \times 10^9 \text{ cm}$ and $t_M = 3000 \text{ yr}$. If t_B is the time scale for the boundary spin-down, then the change $\Delta\Omega$ in Ω across the RS layer is $\Delta\Omega \sim (t_M/t_B)\Omega$. The associated shear in linear velocity is $\theta = R\Delta\Omega/\delta_{RS}$. Thus the Richardson number is roughly given by

$$J = (N/\theta)^2 = (N\delta_{RS}/R\Delta\Omega)^2 = (t_B/t_M)^2. \quad (84)$$

Stability requires $J \geq \frac{1}{4}$, so we expect stability if t_B exceeds $\frac{1}{2}t_M = 1500 \text{ yr}$, which it surely does. Estimates for other instabilities can be made, but it is clear from the above numbers that no appreciable gradients, and hence no instabilities, are to be expected for $t_B \gg t_M$.

For helpful discussions of the spin-down problem and for reading the final manuscript, I thank Dr E. R. Benton, Dr P. A. Clark and Dr J. H. Thomas. I acknowledge many stimulating discussions of spin-down with Dr Takeo Sakurai in the early stages of this work.

REFERENCES

- BARCILON, V. & PEDLOSKY, J. 1967 Linear theory of rotating stratified fluid motions. *J. Fluid Mech.* **29**, 1–16.
- BREThERTON, F. P. & SPIEGEL, E. A. 1968 The effect of the convection zone on solar spin-down. *Astrophys. J. Lett.* **153**, L77–80.
- CLARK, A., CLARK, P. A., THOMAS, J. H. & LEE, N. H. 1971 Spin-up of a strongly stratified fluid in a sphere. *J. Fluid Mech.* **45**, 131–150.
- CLARK, A., THOMAS, J. H. & CLARK, P. A. 1969 Solar differential rotation and oblateness. *Science*, **164**, 290–291.
- DICKE, R. H. 1964 The sun's rotation and relativity. *Nature*, **202**, 432–435.
- DICKE, R. H. 1970 Internal rotation of the Sun. *Ann. Rev. Astron. & Astrophys.* **8**, 297–328.
- FRICKE, K. J. & KIPPENHAHN, R. 1972 Evolution of rotating stars. *Ann. Rev. Astron. & Astrophys.* **10**, 45–72.
- GOLDREICH, P. & SCHUBERT, G. 1967 Differential rotation in stars. *Astrophys. J.* **150**, 571–587.
- GREENSPAN, H. P. & HOWARD, L. N. 1963 On a time-dependent motion of a rotating fluid. *J. Fluid Mech.* **17**, 385–404.

- HOLTON, J. R. 1965 The influence of viscous boundary layers on transient motions in a stratified rotating fluid. part 1. *J. Atmos. Sci.* **22**, 402-411.
- HOWARD, L. N., MOORE, D. W. & SPIEGEL, E. A. 1967 Solar spin-down problem. *Nature*, **214**, 1297-1299.
- MESTEL, L. 1965 Meridional circulation in stars. In *Stellar Structure*, (ed. L. H. Aller & D. B. McLaughlin), pp. 465-497. University of Chicago Press.
- ROXBURGH, I. W. 1965 A note on the boundary of convective zones in stars. *Mon. Not. Roy. Astr. Soc.* **130**, 223-228.
- SAKURAI, T. 1969 Spin-down problem of rotating stratified fluid in thermally insulated circular cylinders. *J. Fluid Mech.* **37**, 689-699.
- SAKURAI, T., CLARK, A. & CLARK, P. A. 1971 Spin-down of a Boussinesq fluid of small Prandtl number in a circular cylinder. *J. Fluid Mech.* **49**, 753-773.
- SCHWARZSCHILD, M. 1958 *Structure and Evolution of the Stars*. Princeton University Press.
- SPIEGEL, E. A. 1972 A history of solar rotation. *Physics of the Solar System* (ed. S. I. Rasool), pp. 61-87. N.A.S.A.
- WALIN, G. 1969 Some aspects of time-dependent motion of a stratified rotating fluid. *J. Fluid Mech.* **36**, 289-307.